Electronic Supplementary Material (ESI) for Nanoscale.

SUPPORTING INFORMATION

Structure and vibrational properties of 1D molecular wires: from graphene to graphdiyne

Francesco De Boni,[†] Roberto Pilot,[†,‡] Alberto Milani,[#] Viktoria V. Ivanovskaya,[†] Raichel J. Abraham,[†] Stefano Casalini,[†] Danilo Pedron, [†] Carlo S. Casari,[#] Mauro Sambi[†,‡] and Francesco Sedona[†,*]

[†] Dipartimento di Scienze Chimiche, Università degli Studi di Padova, Via Marzolo 1, 35131 Padova, Italy
[‡] Consorzio INSTM, Unità di Ricerca di Padova, Padova, Italy
[#] Department of Energy, Politecnico di Milano, via Ponzio 34/3, I-20133 Milano, Italy

* Corresponding author: francesco.sedona@unipd.it

1. Additional details about the synthesis of PPP wires starting from the DBTP precursor: STM images and XPS spectra

Figure S1 shows large-scale STM images of the two-step synthesis of PPP wires starting from the DBTP precursor on Au(111). The room temperature (RT) deposition of DBTP (15 minutes at 120°C) leads to a monolayer of molecules arranged in a checkered pattern (Figure S1a). Subsequent annealing at 200°C produces a high coverage of long PPP wires. Bromine atoms are adsorbed on the gold surface between PPP wires, as distinguishable from the bright contrast in the STM image (Figure S1b).

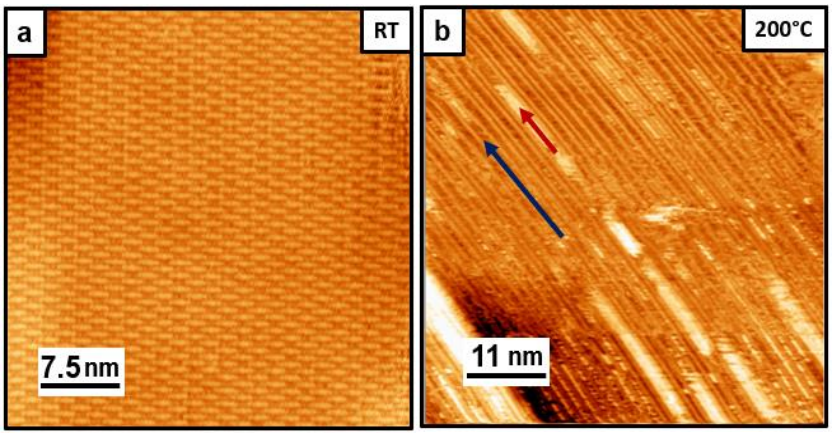

Figure S1 – STM images of the two-step synthesis of PPP wires from the DBTP precursor on Au(111). a) After the RT deposition of DBTP, the checkered pattern of the molecules is visible on the surface (I = 5.9 nA; V = -1.2 V). b) The annealing at 200°C produces long PPP wires following the direction indicated by the blue arrow. Bromine atoms are still present on the surface between the wires (red arrow) (I = 2.5 nA; V = -0.8 V).

C 1s and Br 3d XPS spectra of both DBTP molecules and PPP wires after the annealing at 200°C are reported in Figure S2, confirming the changes in the chemical structure of the overlayer expected during the synthesis.

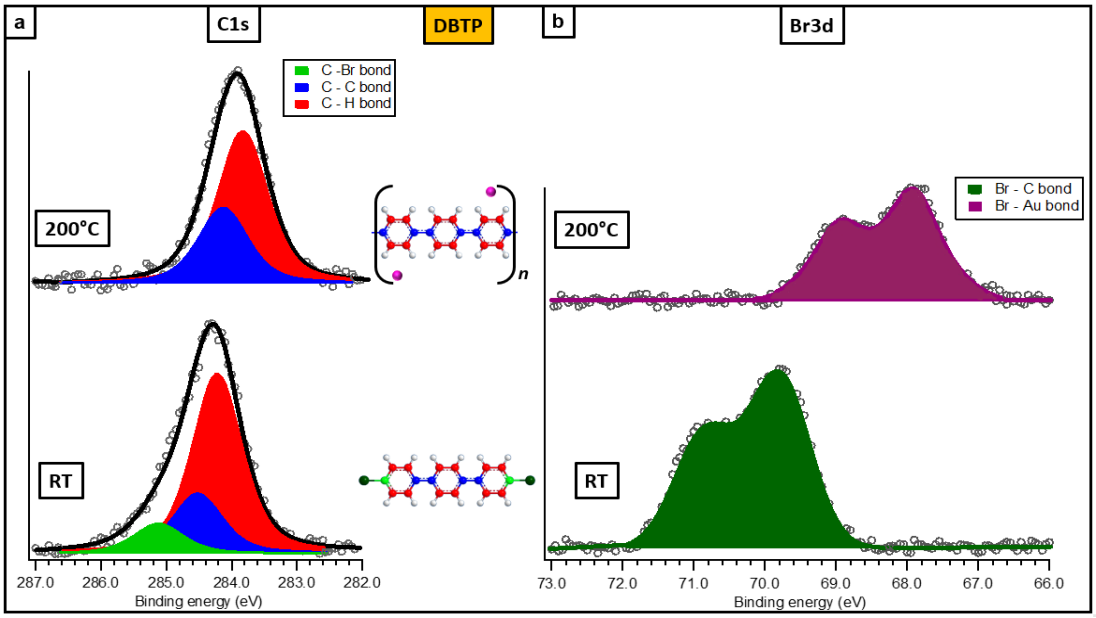

Figure S2 – Fitted (a) C 1s and (b) Br 3d XPS spectra for the two-step synthesis of PPP wires on Au(111). In the central panel, C atoms in the DBTP precursor and in the PPP are colored according to the following color legend: C bonded to Br – light green; C bonded to H – red; C bonded exclusively to C – blue. Instead, Br atoms are represented with the following color legend: Br bonded to C – dark green; Br chemisorbed on Au – violet.

2. XPS parameters of C1s peaks

To evaluate the changes in position, area, and fwhm of the C1s peaks we fitted the experimental spectra with a single component keeping constant the asymmetry parameters on XPSpeak41 software to have consistent parameters. The fitting is reported in figure S3 and the parameter are reported in table S1

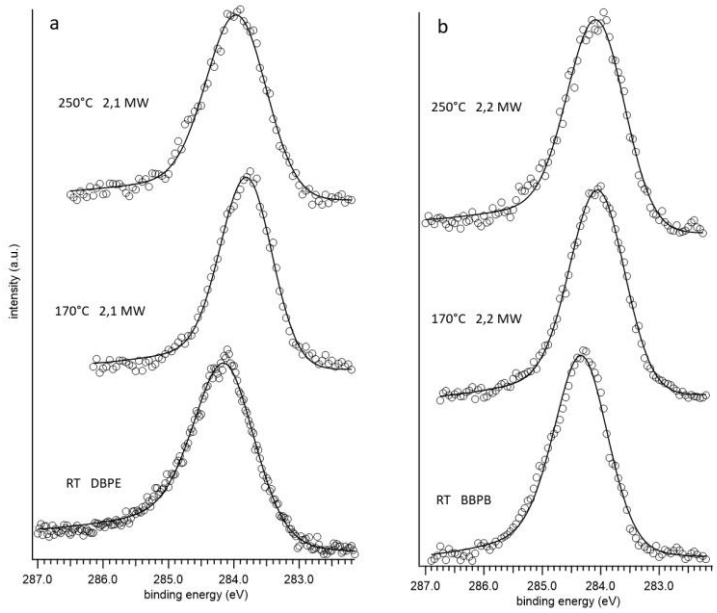

Figure S3. Fitting with a single component of the C1s XPS peaks reported in figure 2 and 3 of the main text.

Table S1 – XPS peak parameters (BE, fwhm, area) of the whole di C 1s peak for each growth step starting from the DBPE and DBPB. The area percentage is calculated relative to the area of the sample at RT, considered as 100%.

	Deposition RT			Annealing 170°C			Annealing 250°C		
	BE [eV]	fwhm(eV)	Area	BE [eV]	fwhm(eV)	Area	BE [eV]	fwhm(eV)	Area
DBPE - 2,1 MW whole C1s peak parameters (figure S3a)	284.1	1.15	100%	283.8	0,95	85%	284.0	1,13	80%
BBPB - 2,2 MW whole C1s peak parameters (figure S3b)	284.3	1.15	100%	284.1	1.14	89%	284.1	1.16	85%

3. XPS fitting parameters: additional details

X-ray Photoelectron Spectroscopy (XPS) spectra were fitted using the XPSPeak41 software (see the Experimental Section of the main article for more information). For each peak, we initially performed the fit by fixing the binding energy (BE) and the percentage area of the different components at the expected values (from the literature). Moreover, we fixed full-width-at-half-maximum (FWHM) and lineshape (Voigt function), in terms of percentage of Lorentzian and Gaussian components, at plausible values (0.7-1 eV range for FWHM, 40-60% range for the Lorentzian component in the lineshape).
Then, we let both BE and percentage area free to vary and carried out the fit again, maintaining the other two parameters fixed. The final result was evaluated by checking the χ^2 parameter: if it was far from 1, which is the correct value for an optimum simulation, all the parameters of the peak were tuned and the fit repeated.

Tables S1, S2, and S3 report the positions (binding energy, BE) and the relative areas of the different C 1s components for each growth step starting from DBPE, DBPB, and DBTP precursors, respectively.

Table S2– XPS peak positions (BE, measured in eV) of the different C 1s components for each growth step starting from the DBPE precursor and the corresponding amount of each component as a percentage of the total peak area.

DBPE		Deposition RT			Annealing 170°C		
Bonds		BE [eV]	Area		BE [eV]	Area	
C-H		284.0	71.1%		283.7	71.3%	
C-C		284.4	14.3%		284.1	28.7%	
C-Br		284.8	14.6%				

Table S3 – XPS peak positions (BE, measured in eV) of the different C 1s components for each growth step starting from the DBPB precursor and the corresponding amount of each component as a percentage of the total peak area.

DBPB		Deposition RT			Annealing 170°C		
Bonds		BE [eV]	Area		BE [eV]	Area	
C-H		284.2	74.7%		284.0	74.9%	
C-C		284.6	12.5%		284.3	25.1%	
C-Br		285.0	12.8%				

Table S4 – XPS peak positions (BE, measured in eV) of the different C 1s components for each growth step starting from the DBTP precursor and the corresponding amount of each component as a percentage of the total peak area.

DBTP		Deposition RT			Annealing 200°C		
Bonds		BE [eV]	Area		BE [eV]	Area	
C-H		284.2	66.9%		283.8	66.4%	
3C-C		284.5	22.0%		284.2	33.6%	
C-Br		285.1	11.1%				

4. Raman experiments: additional details

For each sample, Raman spectra were collected at increasing laser powers on the same point and we did not observe sample degradation. Additionally, measurements were performed on the same sample after 24 hours without any indication of degradation.
In Figure S4, two spectra of PPP MWs are shown. The first was collected with 5 mW (black line) and the second at 50 mW (red line); they were both integrated 20 seconds and averaged out of 10 acquisitions. Spectra have been background subtracted, normalized to the maximum and shifted for better displaying.
The spectra exhibit the same shape, with no change of the band ratios. Moreover, the decomposition of organic molecules is typically accompanied by the formation of carbonaceous materials, with bands around ~1350 cm^{-1}, ~1580 cm^{-1}, and ~1500 cm^{-1} which correspond to the D and G bands of graphite-like compounds, and to amorphous carbon, respectively: these bands are not observed in our case.[1,2]
We can therefore conclude that no sample decomposition occurred during measurements.
Analogous considerations can be drawn for 2,1 GY MW (Figure S5) and 2,2 GY MW (Figure S6).

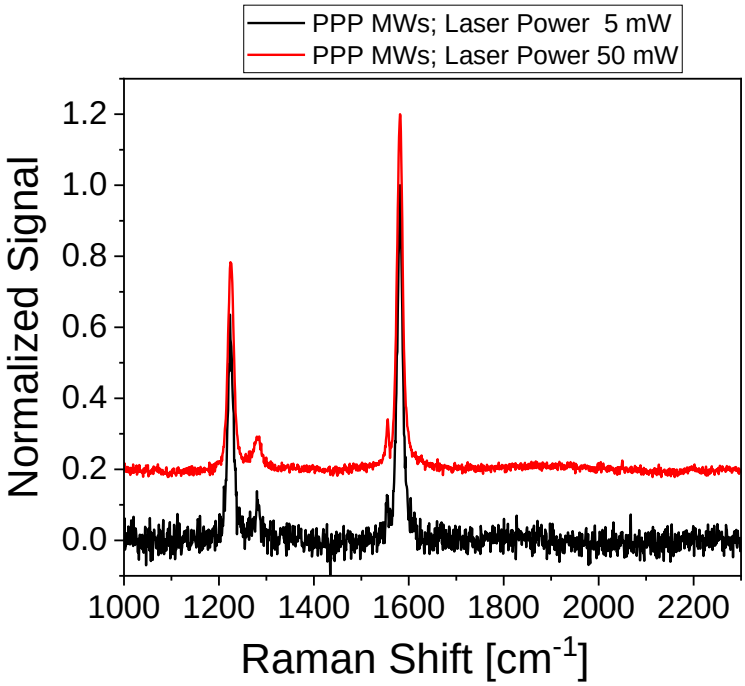

Figure S4 -Raman spectra of PPP MWs recorded on the same point of the sample, first with 5 mW laser power (black line) and then with 50 mW (red line). The integration time was 20 seconds and 10 acquisitions were averaged in both cases. Spectra have been baseline subtracted, normalized to the maximum and vertically displaced for clarity.

[1] A.C. Ferrari and J. Robertson, *Phys. Rev. B*, 2000, **61**, 14095–14107.

[2] R.A. Álvarez-Puebla, *J. Phys. Chem. Lett.*, 2012, **3**, 857–866.

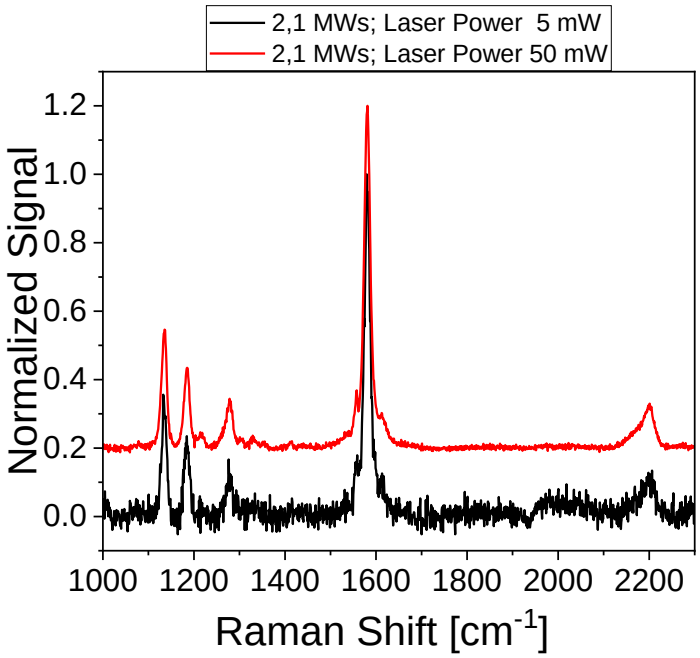

Figure S5. Raman spectra of 2,1 GY MWs recorded on the same point of the sample, first with 5 mW laser power (black line) and then with 50 mW (red line). The integration time was 20 seconds and 10 acquisitions were averaged in both cases. Spectra have been baseline subtracted, normalized to the maximum and vertically displaced for clarity.

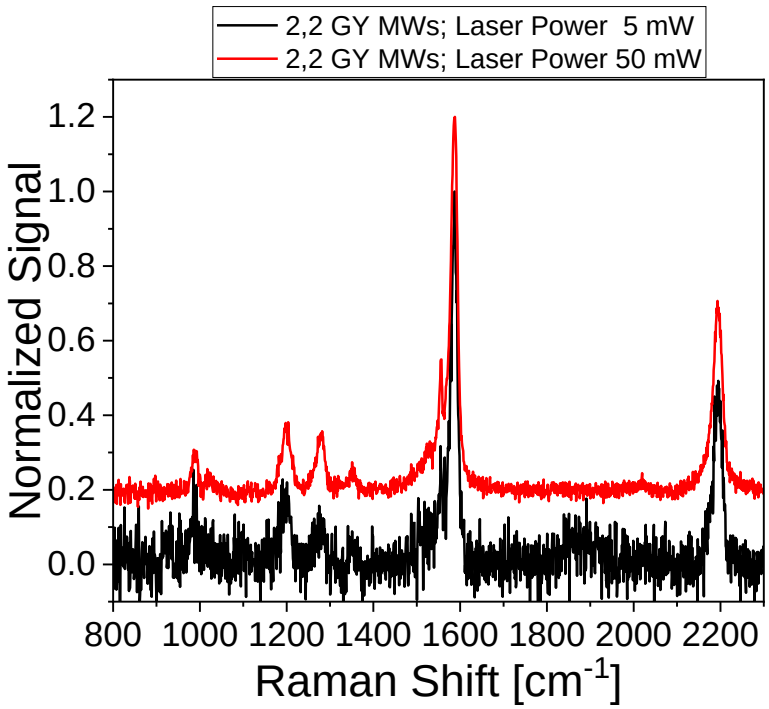

Figure S6. Raman spectra of 2,2 GY MWs recorded on the same point of the sample, first with 5 mW laser power (black line) and then with 50 mW (red line). The integration time was 20 seconds and 10 acquisitions were averaged in both cases. Spectra have been baseline subtracted, normalized to the maximum and vertically displaced for clarity.

Raman measurements of powders were recorded in a standard Micro Raman configuration. Similarly to the previous case, spectra at increasing powers were recorded on the same point of the sample and did show signs of degradation. Data are reported in Figure S7 for DBTP, Figure S8 for DBPE and Figure S9 for BBPB.

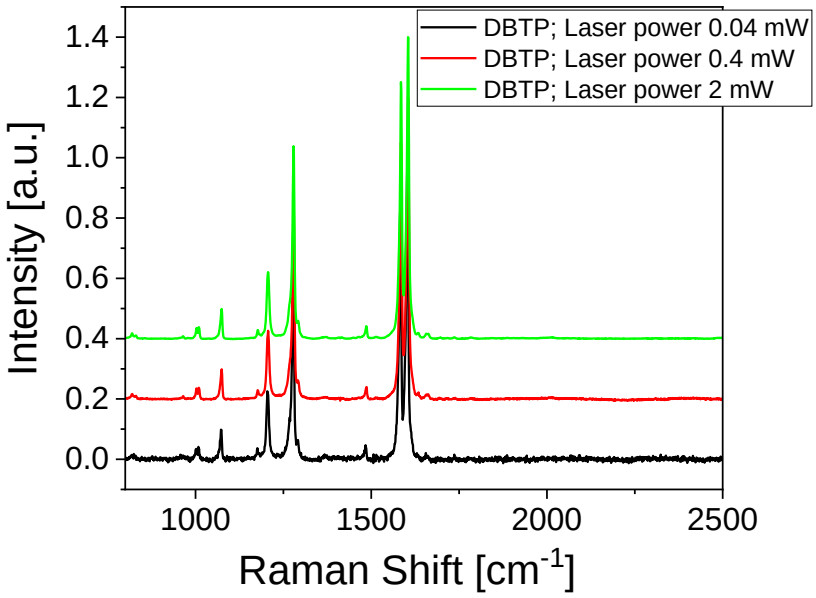

Figure S7. Raman spectra DBTP recorded on the same point of the sample, with 0.04 mW (black line), 0.4 mW (red line) and 2 mW (green line). The integration time was 10 seconds and 10 acquisitions were averaged in all cases. Spectra have been baseline subtracted, normalized to the maximum and vertically displaced for clarity.

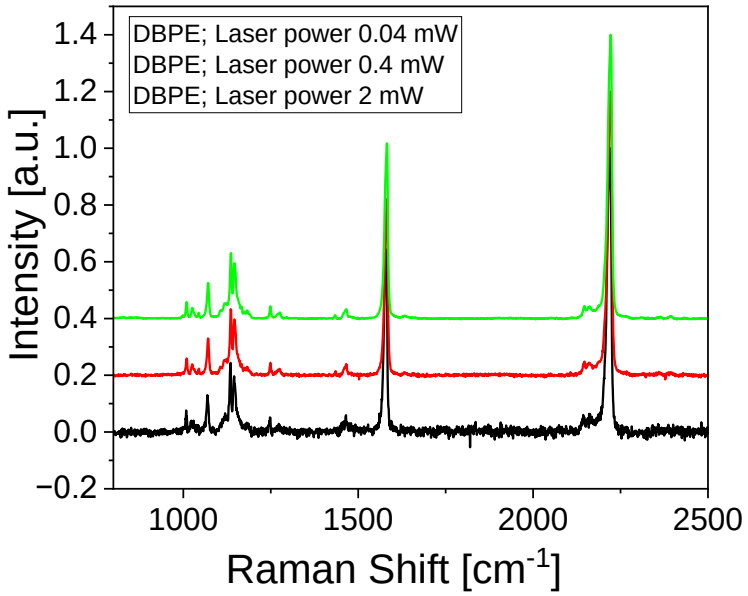

Figure S8.. Raman spectra DBPE recorded on the same point of the sample, with 0.04 mW (black line), 0.4 mW (red line) and 2 mW (green line). The integration time was 10 seconds and 10 acquisitions were averaged in all cases. Spectra have been baseline subtracted, normalized to the maximum and vertically displaced for clarity.

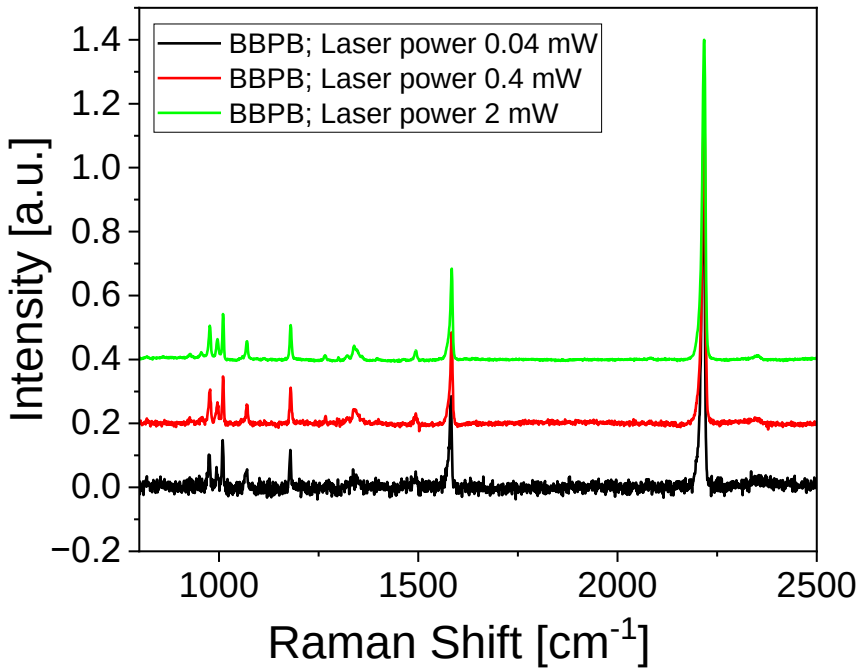

Figure S9. Raman spectra BBPB recorded on the same point of the sample, with 0.04 mW (black line), 0.4 mW (red line) and 2 mW (green line). The integration time was 10 seconds and 10 acquisitions were averaged in all cases. Spectra have been baseline subtracted, normalized to the maximum and vertically displaced for clarity.

5. Simulation of Raman spectra: additional details

In this Paragraph, we report in detail the simulated normal modes of vibration associated with the most significant Raman bands for each nanostructure we discussed in the main article (DBTP, DBPE, and DBPB molecules, and the corresponding polymers).

a) DBTP molecule

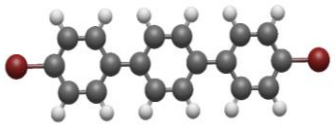

Table S5 – Experimental Raman shift (cm^{-1}), simulated Raman shift (cm^{-1}), and simulated Raman intensity of the normal modes of vibration associated with the first five Raman bands present in the spectrum of DBTP molecular precursor.

	Mode 1	Mode 2	Mode 3	Mode 4	Mode 5
Experimental Raman shift (cm^{-1})	406	777	1006	1074	1206
Simulated Raman shift (cm^{-1})	412	785	1000	1085	1215
Simulated Raman intensity (A^4/amu)	10	45	130	500	2204

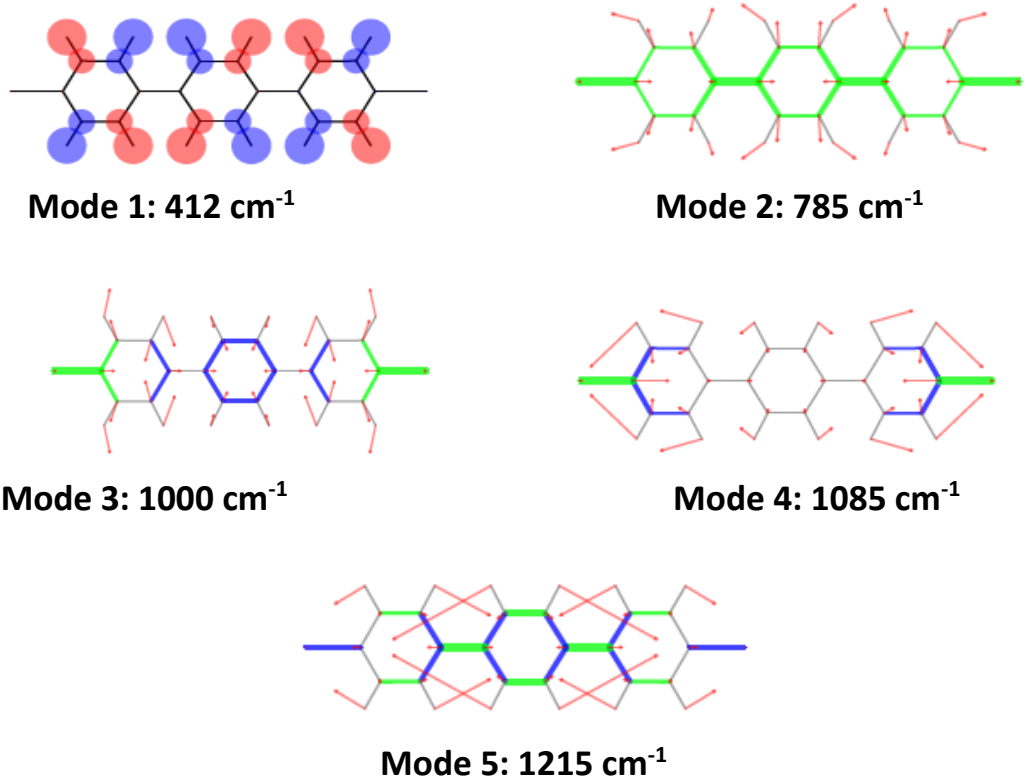

Figure S10.– Sketches of the DFT computed (PBE0/cc-pVTZ) normal modes of vibration associated with the first five Raman bands of DBTP molecular precursor, as discussed in the main article. The values of wavenumbers here indicated are the simulated ones for a planar molecule. Movements of the atoms are represented according to the following legend: red arrows represent bond bending, while colored segments show bond stretching with different vibrational phases depending on the color. The length of the arrows and the width of the segments are proportional to the contribution of each vibration to the whole normal mode.

Table S6 – Experimental Raman shift (cm^{-1}), simulated Raman shift (cm^{-1}), and simulated Raman intensity of the normal modes of vibration associated with the remaining five Raman bands present in the spectrum of the DBTP molecular precursor.

	Mode 6	Mode 7	Mode 8	Mode 9	Mode 10
Experimental Raman shift (cm^{-1})	1280	1486	1585	1605	3065
Simulated Raman shift (cm^{-1})	1267	1480	1585	1610	3054
Simulated Raman intensity (A^4/amu)	4320	478	9934	3013	472

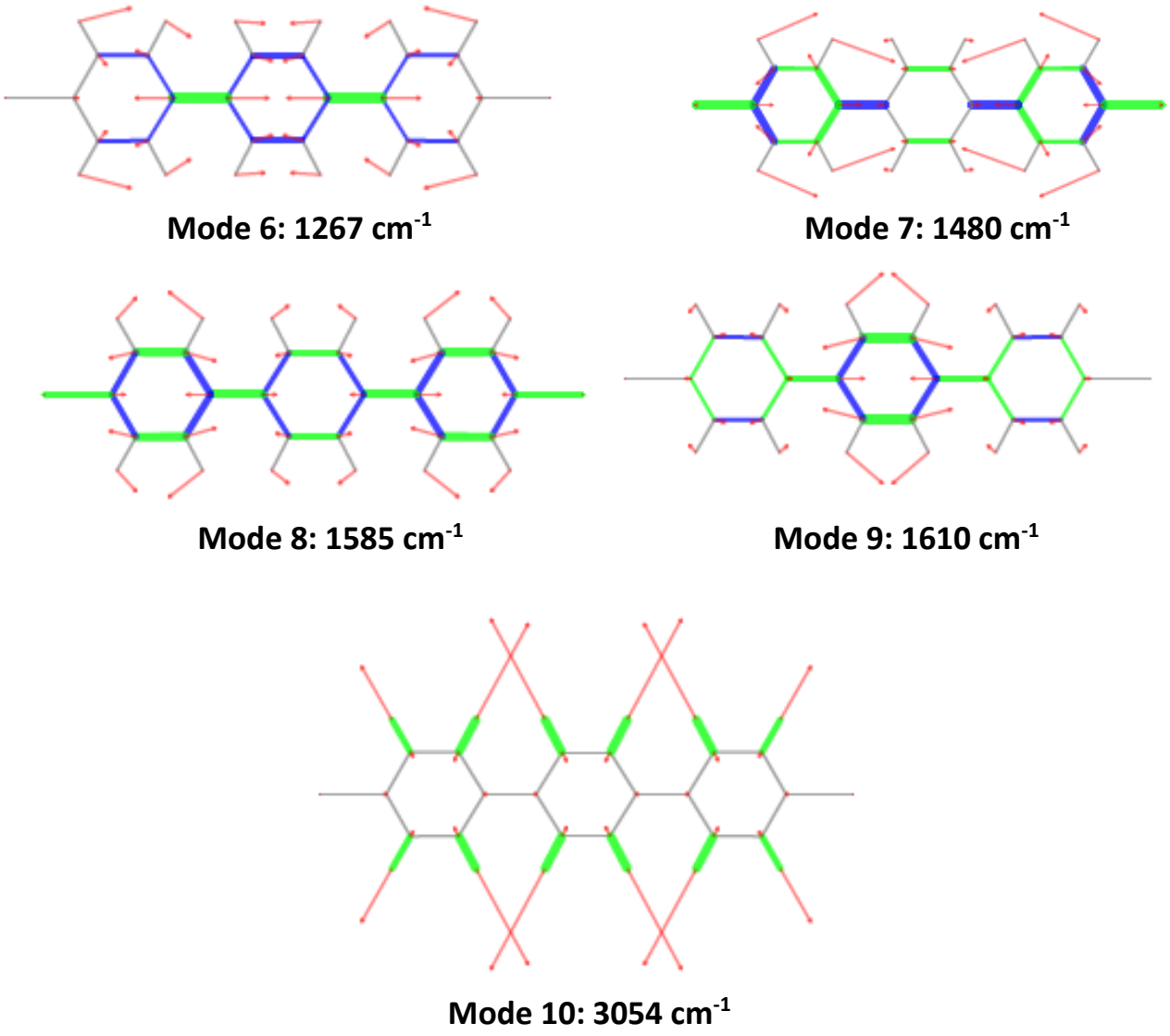

Figure S11. Sketches of the DFT computed (PBE0/cc-pVTZ) normal modes of vibration associated with the remaining five Raman bands of the DBTP molecular precursor, as discussed in the main article. The values of wavenumbers here indicated are the simulated ones for a planar molecule. Movements of the atoms are represented according to the following legend: red arrows represent bond bending, while colored segments show bond stretching with different vibrational phases depending on the color. The length of the arrows and the width of the segments are proportional to the contribution of each vibration to the whole normal mode.

b) DBPE molecule

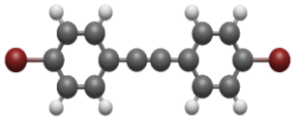

Table S7 – Experimental Raman shift (cm^{-1}), simulated Raman shift (cm^{-1}), and simulated Raman intensity of the normal modes of vibration associated with the first four Raman bands present in the spectrum of DBPE molecular precursor.

	Mode 1	Mode 2	Mode 3	Mode 4
Experimental Raman shift (cm^{-1})	1010	1071	1136	1248
Simulated Raman shift (cm^{-1})	1005	1073	1134	absent
Simulated Raman intensity (A^4/amu)	107	425	2340	absent

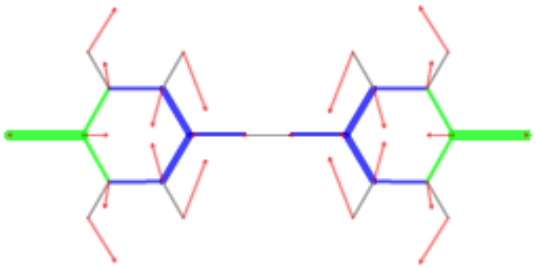

Mode 1: 1005 cm^{-1}

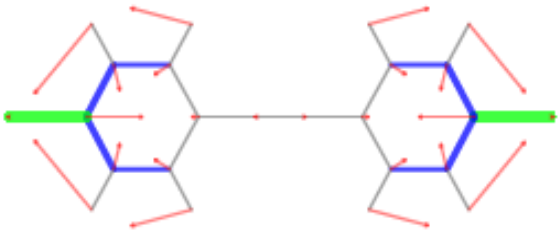

Mode 2: 1073 cm^{-1}

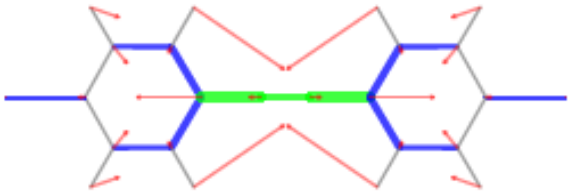

Mode 3: 1134 cm^{-1}

Figure S12. Sketches of the DFT computed (PBE0/cc-pVTZ) normal modes of vibration associated with the first four Raman bands of DBPE molecular precursor, as discussed in the main article. The values of wavenumbers here indicated are the simulated ones for a planar molecule. Movements of the atoms are represented according to the following legend: red arrows represent bond bending, while colored segments show bond stretching with different vibrational phases depending on the color. The length of the arrows and the width of the segments are proportional to the contribution of each vibration to the whole normal mode.

Table S8- Experimental Raman shift (cm^{-1}), simulated Raman shift (cm^{-1}), and simulated Raman intensity of the normal modes of vibration associated with the remaining four Raman bands present in the spectrum of the DBPE molecular precursor.

	Mode 5	Mode 6	Mode 7	Mode 8
Experimental Raman shift (cm^{-1})	1466	1585	2222	3056
Simulated Raman shift (cm^{-1})	1463	1585	2216	3048
Simulated Raman intensity (A^4/amu)	260	5250	17108	133

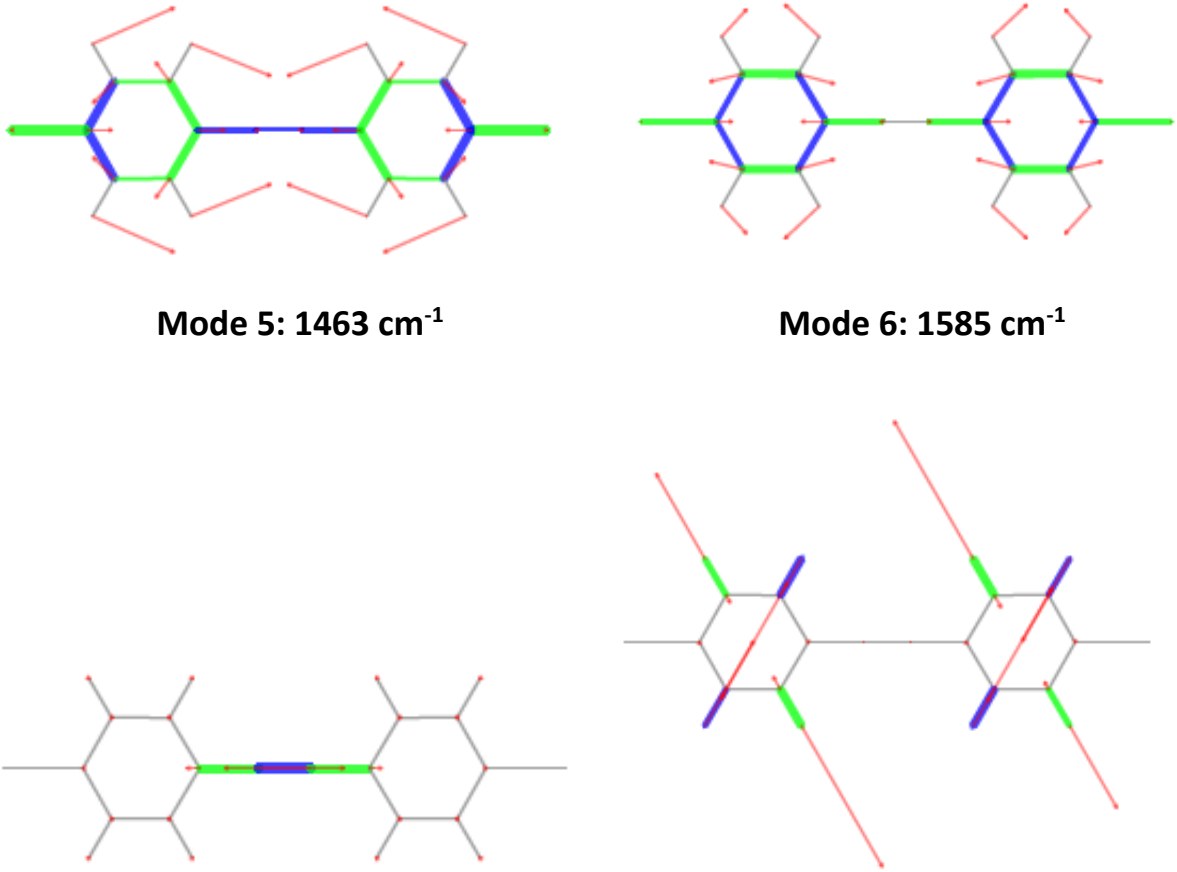

Figure S13. Sketches of the DFT computed (PBE0/cc-pVTZ) normal modes of vibration associated with the remaining four Raman bands of DBPE molecular precursor, as discussed in the main article. The values of wavenumbers here indicated are the simulated ones for a planar molecule. Movements of the atoms are represented according to the following legend: red arrows represent bond bending, while colored segments show bond stretching with different vibrational phases depending on the color. The length of the arrows and the width of the segments are proportional to the contribution of each vibration to the whole normal mode.

c) DBPB molecule

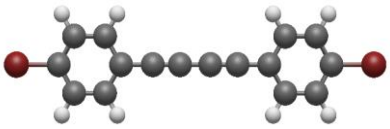

Table S9 – Experimental Raman shift (cm^{-1}), simulated Raman shift (cm^{-1}), and simulated Raman intensity of the normal modes of vibration associated with the first four Raman bands present in the spectrum of the DBPB molecular precursor.

	Mode 1	Mode 2	Mode 3	Mode 4
Experimental Raman shift (cm^{-1})	1010	1070	1180	1340
Simulated Raman shift (cm^{-1})	1010	1075	1166	1345
Simulated Raman intensity (A^4/amu)	1035	280	859	1532

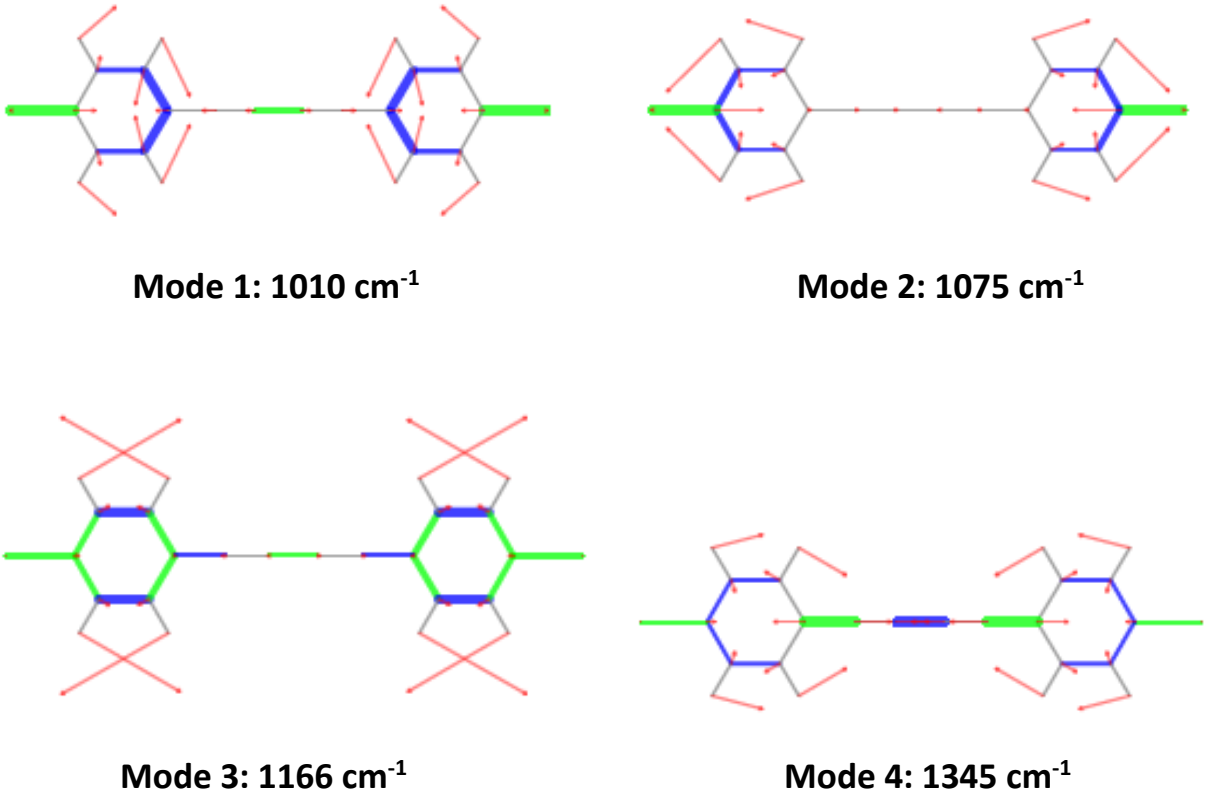

Figure S14. Sketches of the DFT computed (PBE0/cc-pVTZ) normal modes of vibration associated with the first four Raman bands of DBPB molecular precursor, as discussed in the main article. The values of wavenumbers here indicated are the simulated ones for a planar molecule. Movements of the atoms are represented according to the following legend: red arrows represent bond bending, while colored segments show bond stretching with different vibrational phases depending on the color. The length of the arrows and the width of the segments are proportional to the contribution of each vibration to the whole normal mode.

Table S10 – Experimental Raman shift (cm^{-1}), simulated Raman shift (cm^{-1}), and simulated Raman intensity of the normal modes of vibration associated with the remaining four Raman bands present in the spectrum of the DBPB molecular precursor.

	Mode 5	Mode 6	Mode 7	Mode 8
Experimental Raman shift (cm^{-1})	1495	1585	2218	3061
Simulated Raman shift (cm^{-1})	1480	1585	2220	3039
Simulated Raman intensity (A^4/amu)	1089	11619	59467	450

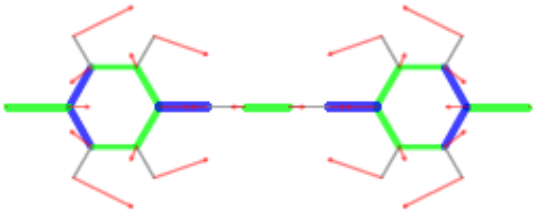

Mode 5: 1480 cm^{-1}

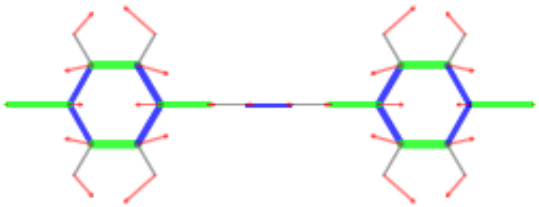

Mode 6: 1585 cm^{-1}

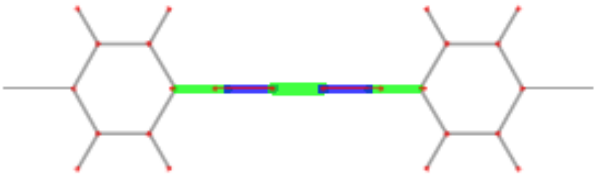

Mode 7: 2220 cm^{-1}

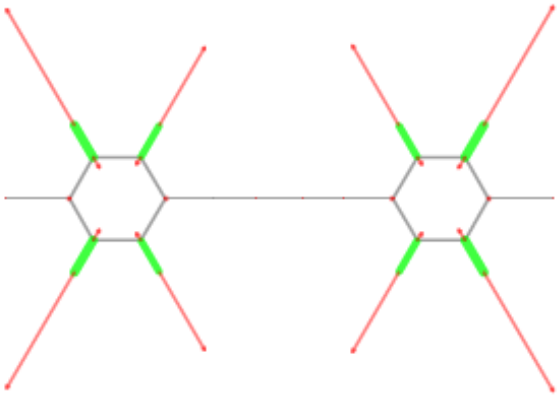

Mode 8: 3039 cm^{-1}

Figure S15 – Sketches of the DFT computed (PBE0/cc-pVTZ) normal modes of vibration associated with the remaining four Raman bands of DBPB molecular precursor, as discussed in the main article. The values of wavenumbers here indicated are the simulated ones for a planar molecule. Movements of the atoms are represented according to the following legend: red arrows represent bond bending, while colored segments show bond stretching with different vibrational phases depending on the color. The length of the arrows and the width of the segments are proportional to the contribution of each vibration to the whole normal mode.

d) PPP wires (DBTP-based polymers)

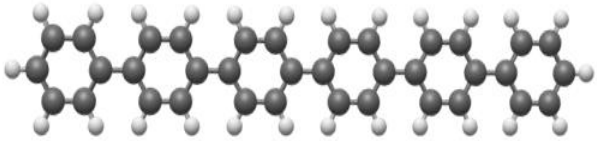

Table S11. Experimental Raman shift (cm^{-1}), simulated Raman shift (cm^{-1}), and simulated Raman intensity of the normal modes of vibration associated with the most significant Raman bands present in the spectrum of PPP wires (DBTP-based polymers).

	Mode 1	Mode 2	Mode 3	Mode 4	Mode 5
Experimental Raman shift (cm^{-1})	805	1222	1276	absent	1583
Simulated Raman shift (cm^{-1})	810	1205	1274	1464	1583
Simulated Raman intensity (A^4/amu)	258	29754	21765	2387	96439

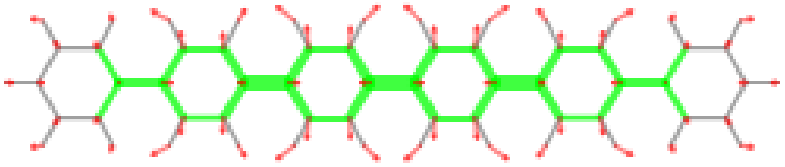

Mode 1: 810 cm^{-1}

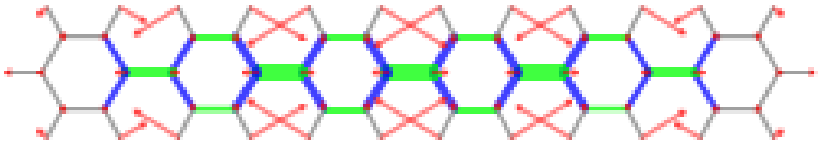

Mode 2: 1205 cm^{-1}

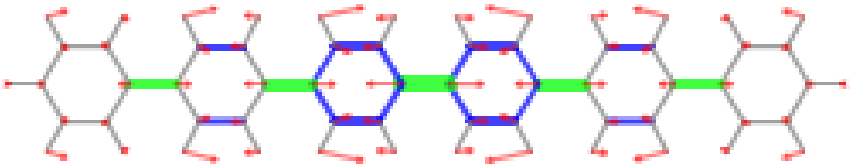

Mode 3: 1274 cm^{-1}

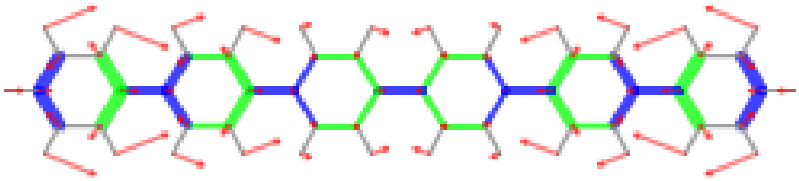

Mode 4: 1464 cm^{-1}

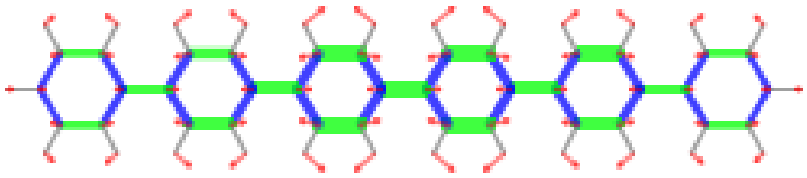

Mode 5: 1583 cm^{-1}

Figure S16. Sketches of the DFT computed (PBE0/cc-pVTZ) normal modes of vibration associated with the most significant Raman bands of PPP wires (DBTP-based polymers), as discussed in the main article. The values of wavenumbers here indicated are the simulated ones for a planar polymer. Movements of the atoms are represented according to the following legend: red arrows represent bond bending, while colored segments show bond stretching with different vibrational phases depending on the color. The length of the arrows and the width of the segments are proportional to the contribution of each vibration to the whole normal mode.

e) 2,1 GY MWs (DBPE-based polymers)

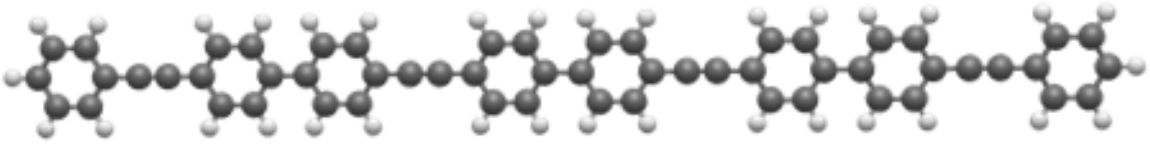

Table S12. Experimental Raman shift (cm^{-1}), simulated Raman shift (cm^{-1}), and simulated Raman intensity of the normal modes of vibration associated with the most significant Raman bands present in the spectrum of 2,1 GY MWs (DBPE-based polymers).

	Mode 1	Mode 2	Mode 3	Mode 4
Experimental Raman shift (cm^{-1})	1137	1278	1582	2205
Simulated Raman shift (cm^{-1})	1130	1260	1582	2193
Simulated Raman intensity (A^4/amu)	116696	73388	442625	434574

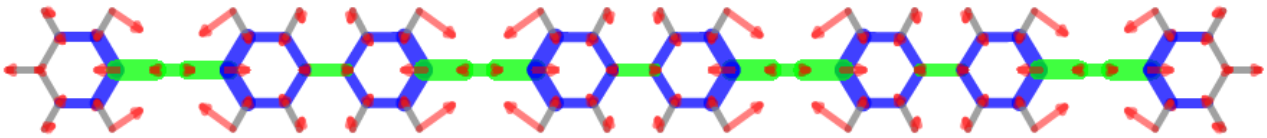

Mode 1: 1130 cm^{-1}

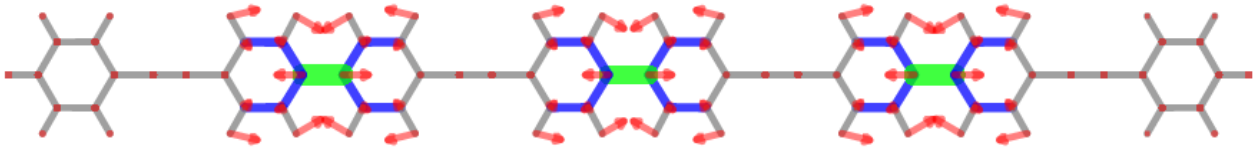

Mode 2: 1260 cm^{-1}

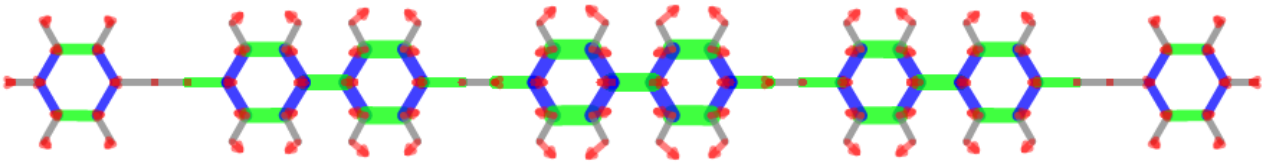

Mode 3: 1582 cm^{-1}

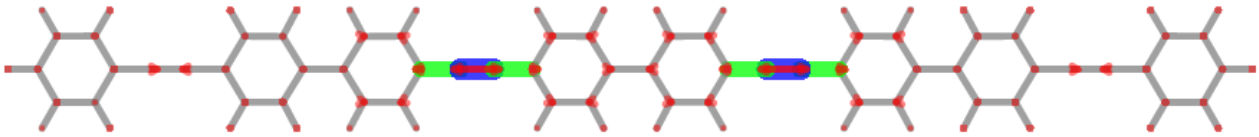

Mode 4: 2193 cm^{-1}

Figure S17. Sketches of the DFT computed (PBE0/cc-pVTZ) normal modes of vibration associated with the most significant Raman bands of 2,1 GY MWs (DBPE-based polymers), as discussed in the main article. The values of wavenumbers here indicated are the simulated ones for a planar polymer. Movements of the atoms are represented according to the following legend: red arrows represent bond bending, while colored segments show bond stretching with different vibrational phases depending on the color. The length of the arrows and the width of the segments are proportional to the contribution of each vibration to the whole normal mode.

f) 2,2 GDY MWs (DBPB-based polymers)

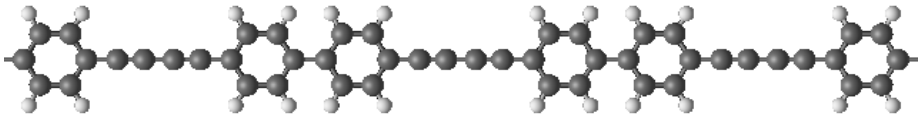

Table S13 – Experimental Raman shift (cm^{-1}), simulated Raman shift (cm^{-1}), and simulated Raman intensity of the normal modes of vibration associated with the most significant Raman bands present in the spectrum of 2,2 GDY MWs (DBPB-based polymers).

	Mode 1	Mode 2	Mode 3	Mode 4	Mode 5	Mode 6
Experimental Raman shift (cm^{-1})	988	1198	1277	1355	1587	2196
Simulated Raman shift (cm^{-1})	987	1196	1265	1358	1586	2205
Simulated Raman intensity (A^4/amu)	30404	53743	86739	58598	605980	1181655

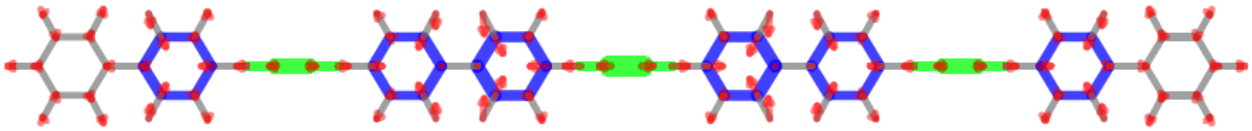

Mode 1: 987 cm^{-1}

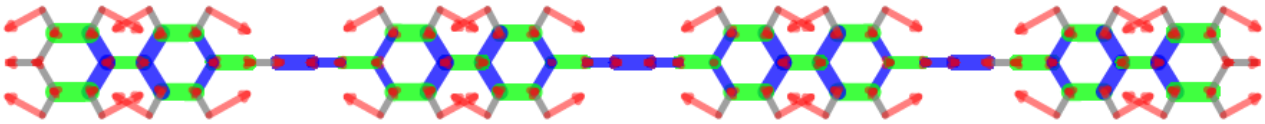

Mode 2: 1196 cm^{-1}

Mode 3: 1265 cm^{-1}

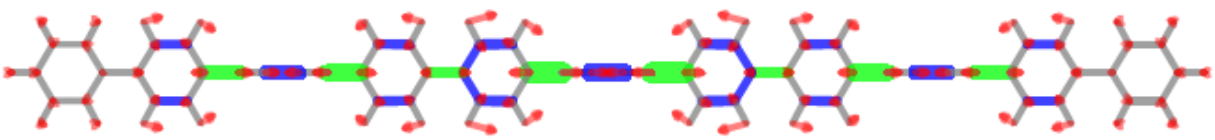

Mode 4: 1358 cm^{-1}

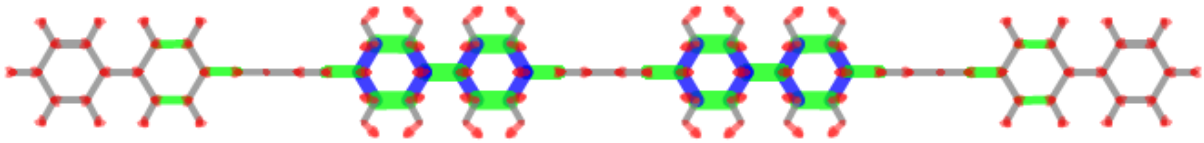

Mode 5: 1586 cm^{-1}

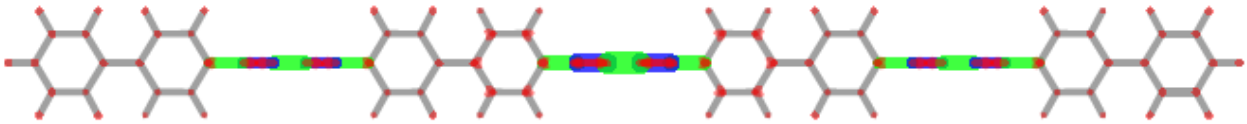

Mode 6: 2205 cm^{-1}

Figure S18. Sketches of the DFT computed (PBE0/cc-pVTZ) normal modes of vibration associated with the most significant Raman bands of 2,2 GDY MWs (DBPB-based polymers), as discussed in the main article. The values of wavenumbers here indicated are the simulated ones for a planar polymer. Movements of the atoms are represented according to the following legend: red arrows represent bond bending, while colored segments show bond stretching with different vibrational phases depending on the color. The length of the arrows and the width of the segments are proportional to the contribution of each vibration to the whole normal mode.

6. Comparison between planar and twisted simulations of polymers Raman spectra

In this Paragraph, we compare the experimental Raman spectrum of the polymers we discussed in the main article (PPP wires, 2,1 GY MWs, and 2,2 GDY MWs) with the corresponding planar and twisted simulations.

a) PPP wires (DBTP-based polymers)

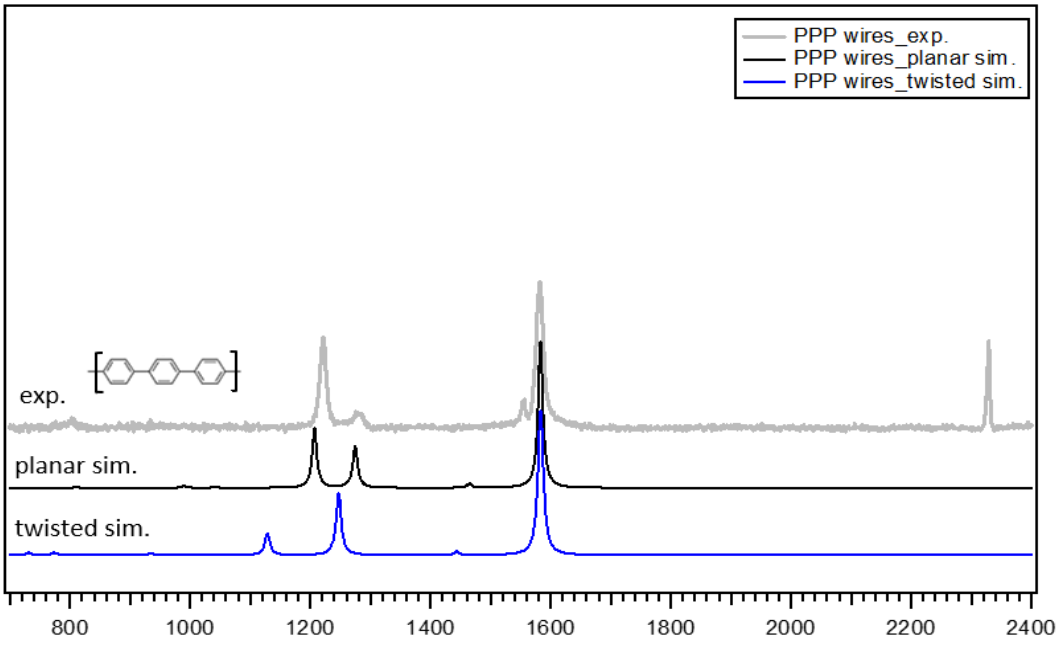

Figure S19. Comparison of the experimental (exp.) Raman spectrum of PPP wires with the corresponding planar (planar sim.) and twisted (twisted sim.) simulations.

b) 2,1 GY MWs (DBPE-based polymers)

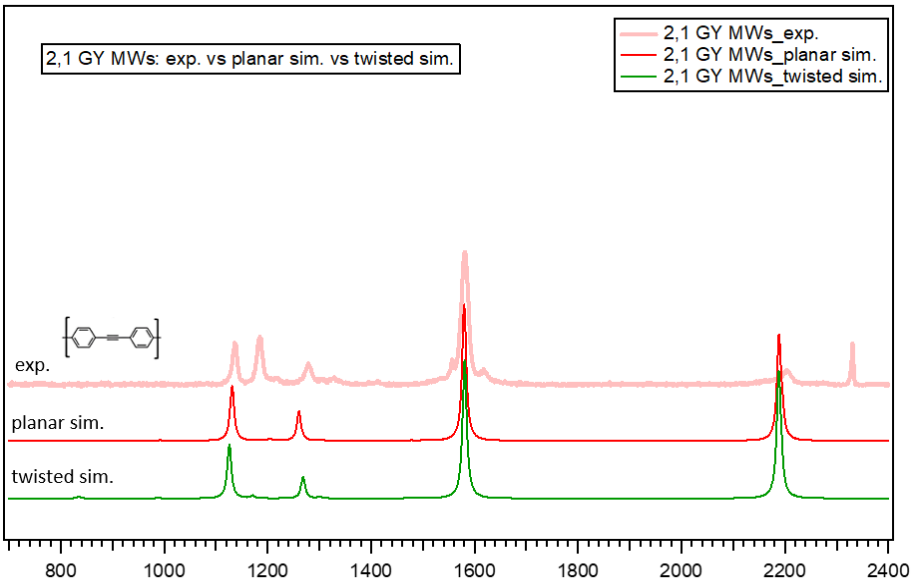

Figure S20. Comparison of the experimental (exp.) Raman spectrum of 2,1 GY MWs with the corresponding planar (planar sim.) and twisted (twisted sim.) simulations.

c) 2,2 GDY MWs (DBPB-based polymers)

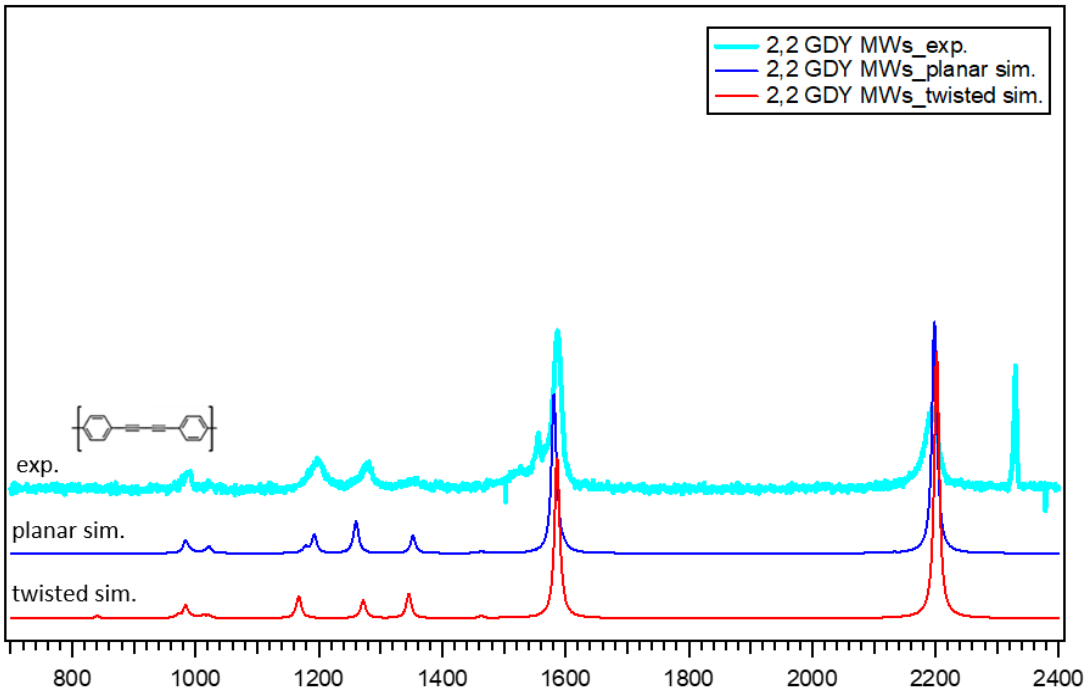

Figure S21. Comparison of the experimental (exp.) Raman spectrum of 2,2 GDY MWs with the corresponding planar (planar sim.) and twisted (twisted sim.) simulations.

7. Stability of the molecular wires after air exposure

We tested the stability of the molecular wires, obtained by thermal treatment at 170°C, exposed to air conditions for 24 hours. Raman spectra showed no significant changes within this time frame. STM measurements on these samples were challenging due to contamination, but we obtained some images in small clean areas where the polymers are clearly visible (see figure S22), confirming their stability.

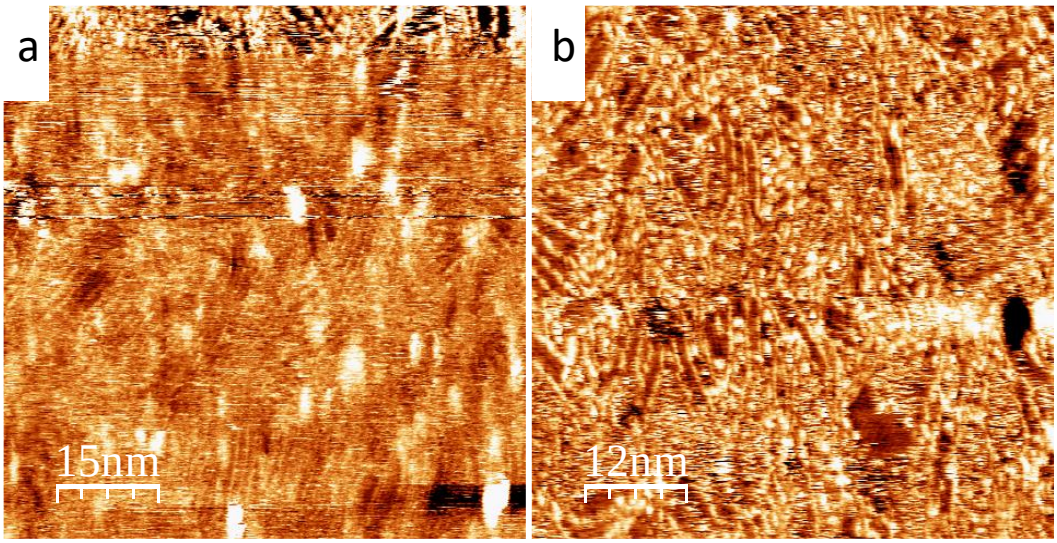

Figure S22. STM images of MWs after 24 hours of exposition to air: a) 2,1MW (V=1.5V I=1.4nA) b) 2,2 MW (V=1.1V I=0.8nA)